Pre-compensation for Anticipated Erasures in LTI Interpolation Systems

Sourav Dey, *Member, IEEE,* Andrew Russell, *Member, IEEE,* and Alan Oppenheim, *Fellow, IEEE*

***Abstract*— This paper considers compensation of anticipated erasures in a discrete-time (DT) signal such that the desired interpolation can still be accomplished, with minimum error, through a linear time-invariant (LTI) filter. The algorithms presented may potentially be useful in the compensation of a fault in a digital-to-analog converter where samples are dropped at known locations prior to reconstruction. We develop four algorithms. The first is a general solution that, in the presence of erasures, minimizes the squared error for arbitrary LTI interpolation filters. In certain cases, e.g. oversampling and a sinc-interpolating filter, we specialize this solution so it perfectly compensates for erasures. The second solution is an approximation to the general solution that computes the optimal, finite-length compensation for arbitrary LTI interpolation filters. The third is a finite-length, windowed version of the oversampled, sinc-interpolating solution using discrete prolate spheroidal sequences. The last is an iterative algorithm in the class of projection onto convex sets. Analysis and results from numerical simulations are presented.**

***Index Terms*— erasures, interpolation, LTI reconstruction, erasure compensation, discrete prolate sphroidal sequences, projection-onto-convex-sets, broken pixels**

EDICS: DSP-RECO Signal Reconstruction or DSP-SAMP Sampling, Extrapolation, and Interpolation

I. Introduction

INTERPOLATING a continuous-time (CT) signal from a discrete-time (DT) representation is an integral part of a variety of techniques for signal processing. In one of the most common forms of interpolation, the DT signal is represented as impulses on a uniformly spaced grid and the interpolation is accomplished by low-pass filtering this uniform impulse train. In most situations, the lowpass filter is fixed. Thus, if erasures occur in the DT signal, without additional compensation, the desired interpolation will be distorted.

For example, consider a system designed for low-pass reconstruction from uniform samples in which, perhaps because of a faulty digital-to-analog (D/A) converter, specific samples are forced to zero. This problem might occur in a flat-panel display with defective pixel LEDs. Such displays inherently rely on a form of low-pass filtering accomplished by viewing the display from an appropriate distance. As illustrated in Figure 6(a), with defective LEDs and without additional compensation, the perceived output is degraded. As we develop in this paper, under certain conditions, it is possible to compensate for the erasures by adjusting the other sample values, and still achieve a suitable reconstruction at the output of a linear time-invariant (LTI) filter.

It is important to note that this problem is not one of data recovery. It is assumed that the correct values of the DT signal are known. It is the conversion process preceding the low-pass filter that forces particular values to zero. In the example of the display, the video card knows the value to transmit to the defective pixel, but the pixel itself cannot display it because it is broken. In anticipation of these erasures, we can change the original DT signal so the distortion after interpolation is reduced.

Manuscript received June 3, 2004; revised December 9, 2004. The associate editor coordinating the review of this manuscript and approving it for publication was Dr. Fredrik Gustafsson.

S. Dey, A. Russell, and A. Oppenheim are with the Digital Signal Processing Group in the Department of Electrical Engineering and Computer Science, Massachusetts Institute of Technology, Room 36-615, 77 Massachusetts Avenue, Cambridge, MA 02139 USA (e-mail: sdey@mit.edu; air@alum.mit.edu; avo@mit.edu)

II. Problem Statement

Mathematically, the problem can be viewed as one of sampling grid conversion. Consider a discrete-time (DT) representation, $x[n]$, on a uniform grid $\mathcal{I}$,

$$\mathcal{I} = \{0, \pm 1, \pm 2, \pm 3, \ldots\}$$

such that conversion to a uniform impulse train with spacing T and interpolation using a filter, $h(t)$, returns our desired continuous-time (CT) signal $r(t)$,

$$r(t) = \sum_{n \in \mathcal{I}} x[n] h(t - nT) \tag{1}$$

It should be emphasized that $x[n]$ is not restricted to being samples of a function. Compensation of the erasure pertains only to the interpolation of a CT signal from a DT representation.

Because of the erasure, we are forced to represent the signal on a non-uniform grid, $\mathcal{I}'$, that is the grid $\mathcal{I}$ with one point removed. For convenience, and without loss of generality, we choose $n = 0$ as the erasure point so that

$$\mathcal{I}' = \{\pm 1, \pm 2, \pm 3, \ldots\}$$

Our goal is to find a DT representation, $\hat{x}[n]$, on the non-uniform grid, $\mathcal{I}'$, that minimizes the squared interpolation error. Specifically, we desire an interpolation $\hat{r}(t)$,

$$\hat{r}(t) = \sum_{n \in \mathcal{I}'} \hat{x}[n] h(t - nT) \tag{2}$$

that minimizes the energy of the error,

$$\mathcal{E}^2 = \int_{-\infty}^{\infty} |\hat{r}(t) - r(t)|^2 dt = \int_{-\infty}^{\infty} |e(t)|^2 dt \tag{3}$$

where $e(t) = \hat{r}(t) - r(t)$. We can equivalently express (2) as

$$\hat{r}(t) = \sum_{n=-\infty}^{\infty} \hat{x}[n]h(t - nT) \tag{4}$$

if we impose the additional constraint that $\hat{x}[0] = 0$. For convenience, we define $\hat{x}[n] - x[n] = c[n]$, or equivalently, $\hat{x}[n] = x[n] + c[n]$. Combining (1), (4), and our definition of $c[n]$, $e(t)$ can be expressed as an expansion in the basis $\{h(t - nT)\}$,

$$e(t) = \sum_{n=-\infty}^{\infty} c[n]h(t - nT) \tag{5}$$

with the constraint $c[0] = -x[0]$. We can equivalently rewrite equation (3),

$$\mathcal{E}^2 = \int_{-\infty}^{\infty} \left(\sum_{n=-\infty}^{\infty} c[n]h(t - nT) \right)^2 dt \tag{6}$$

The objective then is to determine $c[n]$ for $n \neq 0$ that minimizes $\mathcal{E}^2$. It is important to note that expressing $\hat{x}[n]$ in this form of $x[n]$ with additive compensation $c[n]$ is not restrictive, both in the general case and in our further development where we impose certain additional restrictions on $\hat{x}[n]$. While in this paper we only consider full erasure, we can generalize to the case where the affected value is fixed to any constant value, $\hat{x}[0] = C$. In this case, the constraint on the compensation is $c[0] = -x[0] + C$. For convenience, and without loss of generality, we focus exclusively on the case where $C = 0$, corresponding to full erasure.

If $\{h(t - nT)\}$ forms an orthogonal set, e.g the shift-orthogonal sinc-interpolating kernel or B-splines, then by Parseval's relation,

$$\int_{-\infty}^{\infty} |e(t)|^2 dt = T \sum_{n=-\infty}^{\infty} |c[n]|^2 \tag{7}$$

The scaling on the right side of (7) assumes that $\|h(t - nT)\|_2 = T^2$, as is standard in sampling theory. Note that in the orthogonal case from (7), the error is the energy of $c[n]$. Since the value of $c[0]$ is constrained, the optimal compensation signal is

$$c[n] = -x[0]\delta[n] \tag{8}$$

This is a degenerate solution, equivalent to not compensating the erasure. Consequently, non-trivial solutions are possible only if $\{h(t - nT)\}$ is not an orthogonal set.

In Section 3 of this paper, we discuss the general solution to the problem, where $h(t)$ is an arbitrary LTI filter and all values of $x[n]$ may be adjusted. In Section 4, we focus on the case where $h(t)$ is bandlimited and derive solutions that compensates with zero error for the case of an oversampled, sinc-interpolating filter (LPF). In Section 5, we consider the case in which only a finite number of values may be adjusted, and we derive the optimal solution for arbitrary LTI interpolation filters. Sections 6 and 7 present two alternatives for finite-length compensation, a heuristic solution that is an approximation to the optimal solution and an iterative algorithm which converges to the optimal solution for oversampled, sinc-interpolating filters. Lastly, in Section 8, we discuss how the algorithms developed may be use to compensate an image with pixels that are permanently set to zero.

III. General Solution

In this section we derive the optimal compensation for arbitrary LTI interpolation filters $h(t)$. We first focus on the case of a single erasure. In that case, the solution can be computed by minimizing the objective function (6) subject to the constraint $p = c[0] + x[0] = 0$, using the method of Lagrange multipliers. Defining the Lagrangian $q = \mathcal{E}^2 + \lambda p$ and setting to zero the partial derivatives with respect to $c[k]$ for all $k \neq 0$,

$$\frac{\partial}{\partial c[k]} q = \int_{-\infty}^{\infty} 2 \left(\sum_{n=-\infty}^{\infty} c[n]h(t - nT) \right) h(t - kT) \tag{9}$$

$$= 2 \sum_{n=-\infty}^{\infty} c[n] \left(\int_{-\infty}^{\infty} h(t - nT)h(t - kT)dt \right) = 0 \tag{10}$$

which simplifies to,

$$\sum_{n=-\infty}^{\infty} c[n]\phi_{hh}((k - n)T) = 0 \tag{11}$$

where $\phi_{hh}(\tau)$ is the CT deterministic autocorrelation of the filter $h(t)$, defined as

$$\phi_{hh}(\tau) = \int_{-\infty}^{\infty} h(t)h(t - \tau)dt \tag{12}$$

For $k = 0$, the derivative has an extra term with λ', the Lagrange multiplier. Specifically,

$$\frac{\partial}{\partial c[0]} q = 2 \sum_{n=-\infty}^{\infty} c[n]\phi_{hh}(-nT) + \lambda' = 0 \tag{13}$$

Eqs. (11) and (13) can be combined into a single condition (14), where all the constant terms have been incorporated into $\lambda = -\frac{1}{2}\lambda'$.

$$\sum_{n=-\infty}^{\infty} c[n]\phi_{hh}((k - n)T) = \lambda\delta[k] \tag{14}$$

The second derivative in both cases reduces to,

$$\frac{\partial^2}{\partial c[k]^2} q = 2 \int_{-\infty}^{\infty} |h(t - kT)|^2 dt = 2\phi_{hh}(0) \tag{15}$$

which is always positive, ensuring that the optimization finds a minimum. Since n and k are integers, the values $\phi_{hh}((n-k)T)$ are uniform samples of the CT autocorrelation $\phi_{hh}(\tau)$. If we define a DT sequence $\phi_{hh}[n] = \phi_{hh}(nT)$ of the uniform samples, equation (14) can then be expressed in the frequency domain as (16), where $\Phi_{hh}(e^{j\omega})$ is the discrete-time Fourier transform (DTFT) of $\phi_{hh}[n]$. Note that since $h(t)$ is not restricted to be bandlimited, $\Phi_{hh}(e^{j\omega})$ in general has aliased components. We should also note that when $h(t)$ is not bandlimited to π/T, $\phi_{hh}[n] \neq \sum_m h[m]h[m-n]$, the DT autocorrelation of the sampled filter $h[n] = h(nT)$.

Incorporating the constraint $c[0] = -x[0]$, the Lagrange optimization reduces to two equations in the frequency domain,

$$C(e^{j\omega})\Phi_{hh}(e^{j\omega}) = \lambda \tag{16}$$

$$\frac{1}{2\pi}\int_{<2\pi>} C(e^{j\omega})d\omega = -x[0] \tag{17}$$

where λ and $C(e^{j\omega})$ are the unknowns. In the case where, $\Phi_{hh}(e^{j\omega}) \neq 0, \forall\omega$ and the integral, $\kappa = \int_{-\infty}^{\infty} \frac{1}{\Phi_{hh}(e^{j\omega})}d\omega$ converges, these two equations have a unique solution,

$$C_{\text{opt}}(e^{j\omega}) = \frac{-x[0]/\kappa}{\Phi_{hh}(e^{j\omega})} \tag{18}$$

In the case where $\exists\omega : \Phi_{hh}(e^{j\omega}) = 0$, the solution is not unique and cannot be represented by (18). In this important case, where $\Phi_{hh}(e^{j\omega})$ has zeros on the unit circle, the optimal solutions compensate perfectly with zero error. We can derive the optimal solution by inspection, expressing the error (6) in the frequency domain. To express (6) in the frequency domain, we first expand the square and define a new signal $k[n]$,

$$\mathcal{E}^2 = \int_{-\infty}^{\infty}\left(\sum_n\sum_m c[n]c[m]h(t-nT)h(t-mT)\right)dt \tag{19}$$

$$= \sum_n\sum_m c[n]c[m]\left(\int_{-\infty}^{\infty} h(t-nT)h(t-mT)dt\right) \tag{20}$$

$$= \sum_n c[n]\underbrace{\left(\sum_m c[m]\phi_{hh}[n-m]\right)}_{k[n]} \tag{21}$$

$K(e^{j\omega})$, the DTFT of $k[n]$, can be expressed as,

$$K(e^{j\omega}) = C(e^{j\omega})\Phi_{hh}(e^{j\omega}) \tag{22}$$

Eq. (21) is the inner-product of $c[n]$ and $k[n]$. Using Plancherel's theorem for DT sequences [1], we can express (21) in frequency domain as,

$$\mathcal{E}^2 = \int_{<2\pi>} C(e^{j\omega})K^*(e^{j\omega})d\omega \tag{23}$$

$$= \int_{<2\pi>} |C(e^{j\omega})|^2\Phi_{hh}(e^{j\omega})d\omega \tag{24}$$

where $\Phi^*_{hh}(e^{j\omega}) = \Phi_{hh}(e^{j\omega})$ because $\phi_{hh}[n]$ is even and symmetric. If $c[n]$ has frequency components only where $\Phi_{hh}(e^{j\omega}) = 0$, while meeting the constraint $c[0] = -x[0]$, it results in perfect compensation with zero error. A particularly simple solution is a pair of impulses, i.e. if $\Phi_{hh}(e^{j\omega_z}) = 0$ then,

$$C_{\text{opt}}(e^{j\omega}) = -x[0]\pi\left(\delta(\omega-\omega_z)+\delta(\omega+\omega_z)\right) \tag{25}$$

is a solution that compensates with zero error.

Generalization to multiple erasures requires constrained minimization with multiple constraints. For example, assume that there are two erasures at indices n_1 and n_2. The erasures specify two constraints,

$$p_1 = c[n_1] + x[n_1] = 0 \tag{26}$$
$$p_2 = c[n_2] + x[n_2] = 0$$

As before, we minimize $\mathcal{E}^2$ subject to these constraints. Defining the Lagrangian $q = \mathcal{E}^2 + \lambda'_1 p_1 + \lambda'_2 p_2$ and setting to zero the partial derivatives with respect to $c[k]$ for all k results in a condition of the form,

$$\sum_{n=-\infty}^{\infty} c[n]\phi_{hh}((k-n)T) = \lambda_1\delta[k-m_1]+\lambda_2\delta[k-m_2] \tag{27}$$

where $\lambda_1 = -\frac{1}{2}\lambda'_1$ and $\lambda_2 = -\frac{1}{2}\lambda'_2$. In the frequency domain (27) can be expressed as,

$$C(e^{j\omega})\Phi_{hh}(e^{j\omega}) = \lambda_1 e^{-j\omega m_1} + \lambda_2 e^{-j\omega m_2} \tag{28}$$

As in the single-sample case, if $\Phi_{hh}(e^{j\omega}) \neq 0, \forall\omega$ then a unique solution to (28) exists. If $\exists\omega_1, \omega_2 : \Phi_{hh}(e^{j\omega_1}) = 0, \Phi_{hh}(e^{j\omega_2}) = 0, |\omega_1| \neq |\omega_2|$, then solutions that compensate with zero error exist. The exact form of the multiple-erasure perfect compensation solutions are explored in the following section. Both of these solutions, the unique one and the perfect one, generalize to N erasures in a straightforward manner.

IV. Bandlimited Solutions

In this section, we focus on the special case where $e(t)$ is bandlimited and $h(t)$ is a band-limiting filter with $H(j\omega) = 0$ for $\omega > \pi/T$. In this case, by Parseval's relation, there is perfect norm equivalence between CT and DT and the error can be determined directly in the discrete-time domain,

$$\int_{-\infty}^{\infty}|e(t)|^2dt = T\sum_{n=-\infty}^{\infty}|e[n]|^2 \tag{29}$$

Where $e[n] = e(nT)$ is samples of $e(t)$, expressed as $c[n]$ filtered by $h[n] = h(nT)$, a sampled representation of the interpolation filter $h(t)$,

$$e[n] = e(nT) = \sum_{k=-\infty}^{\infty} c[k]h(T(n-k)) = \sum_{k=-\infty}^{\infty} c[k]h[n-k] \tag{30}$$

In this case, the entire problem can be posed in DT. Combining (30), (29), and (3), our error metric reduces in the frequency domain to

$$\mathcal{E}^2 = \frac{T}{2\pi}\int_{<2\pi>}|H(e^{j\omega})C(e^{j\omega})|^2d\omega \tag{31}$$

This expression in analogous to (24), except since $h(t)$ is band-limited, $\Phi_{hh}(e^{j\omega}) = |H(e^{j\omega})|^2$, where $H(e^{j\omega})$ is the DTFT of the sampled CT filter $h[n] = h(nT)$. If $\forall\omega, H(e^{j\omega}) \neq 0$ the optimal solution for the band-limited case is,

$$C_{\text{opt}}(e^{j\omega}) = \frac{-x[0]/\kappa}{|H(e^{j\omega})|^2} \tag{32}$$

where $\kappa = \int_{-\infty}^{\infty}\frac{1}{|H(e^{j\omega})|^2}d\omega$. The solution (32) precludes an important special case: the classical sampling model where $x[n]$ are samples of a band-limited function and $h(t)$ is an ideal low-pass, sinc-interpolating filter with a guard-band.

Specifically, let $x(t)$ be a band-limited, continuous-time signal that is at least slightly oversampled. In addition, we assume that $1/T = R\Omega_c/\pi$, where $x(t)$ is band-limited to Ω_c and $R > 1$ is the oversampling ratio. We denote the ratio

π/R by γ. $x(t)$ is represented by its samples $x[n] = x(nT)$ on the uniform grid $\mathcal{I}$. Low-pass filtering the scaled impulse-train $p(t) = \sum_{n=-\infty}^{\infty} x[n]\delta(t - t_n)$ through $h(t)$ gives our desired interpolation $r(t)$, where $h(t) = \frac{\sin(\Omega_c t)}{\pi t}$ is the impulse response of an ideal, sinc-interpolating filter with cutoff Ω_c. Note that because of oversampling, $\Omega_c < \pi/T$ so $\{h(t-nT)\}$ is not an orthogonal set. Since $h(t)$ is bandlimited, we can pose the problem in DT. In this case, $h[n] = h(nT)$, an ideal DT sinc-interpolating filter with cutoff $\gamma = \Omega_c T = \pi/R$ and gain $1/T$. Without loss of generality, we normalize the time and frequency axes such that $T = 1$ and $\Omega_c = \pi/R$.

Proceeding analogously to the previous section, we can find a solution that compensates with zero error. According to (31), minimizing the energy of $e[n]$ is equivalent to minimizing the energy of $C(e^{j\omega})$ in the pass-band $[-\gamma,\gamma]$ of the interpolation filter $H(e^{j\omega})$. If $c[n]$ has no frequency components for $|\omega| < \gamma$, while meeting the constraint $c[0] = -x[0]$, it results in perfect compensation with zero error. There are an unlimited number of signals that meet this criteria. A particularly simple solution is,

$$c_{\text{ideal}}[n] = -x[0](-1)^n \tag{33}$$

in which case $C_{\text{ideal}}(e^{j\omega})$ is an impulse at $\omega = \pi$. In theory, this solution only requires that $R = 1+\epsilon$, where ϵ is non-zero but otherwise arbitrarily small. More broadly, it can be shown in a straightforward manner that any high-pass signal $c[n]$, that meets the constraint $\frac{1}{2\pi}\int_{-\pi}^{\pi} C(e^{j\omega})d\omega = -x[0]$, with no frequency components for $|\omega| < \gamma$ is a solution.

For a fixed amount of oversampling, perfect compensation can be extended to multiple erasures. The problem is nominally more difficult because there are multiple constraints to satisfy. For example, with two erasures at indices i and j, perfect compensation can be of the form,

$$c[n] = \alpha_1 c_1[n-i] + \alpha_2 c_2[n-j] \tag{34}$$

Where $c_1[n]$ and $c_2[n]$ are perfect compensation sequences for the erasures at i and j, respectively. Imposing the constraints $c[i] = -x[i]$ and $c[j] = -x[j]$, we define a 2×2 system of linear equations that can be solved for the scale factors, α_1 and α_2,

$$\alpha_1 c_1[0] + \alpha_2 c_2[i-j] = -x[i] \tag{35}$$
$$\alpha_1 c_1[j-i] + \alpha_2 c_2[0] = -x[j] \tag{36}$$

For a guard-band of size $\epsilon > 0$, we can always choose $c_1[n]$ and $c_2[n]$ such that these linear equations are non-singular. In fact, we can always choose sinusoids of different frequencies such that the resulting linear equations have a unique solution. For example, in the 2×2 case, we can choose $c_1[n] = \cos[\pi n]$ and $c_2[n] = \cos[(\pi - \frac{\epsilon}{2})n]$. Thus, in the case of an ideal LPF with a guardband, compensating N erasures requires solving an $N \times N$ system of linear equations for the scale factors. The error remains zero because the sum of band-limited signals is also band-limited, i.e. the space of finite-energy band-limited signals is closed. This reasoning can also be used to extend the perfect solutions for the general case, where $h(t)$ is not bandlimited, to compensate for multiple erasures.

V. Optimal Finite Approximation

While the solutions of Section 3 and 4 are optimal and some even result in zero error, they typically have infinite length. In addition, computation of the filter inverse generally requires additional complex calculations in the form of spectral factorization. Consequently, optimal compensation is impractical to implement.

In this section, to mitigate these problems, we design $c[n]$ with the constraint of finite length. The solution we develop is general and applicable when $h(t)$ is an arbitrary LTI filter. We impose the constraint that

$$\hat{x}[n] = x[n], \quad n \neq \mathcal{N} \tag{37}$$

where $\mathcal{N}$ is the finite set of points to be adjusted. This is equivalent to restricting the compensation signal, $c[n]$, to be non-zero only for $n \in \mathcal{N}$. In general, the set $\mathcal{N}$ may be non-sequential, but for simplicity, we focus on symmetric sequential compensation where $\mathcal{N} = [-\frac{N-1}{2}, \frac{N-1}{2}]$. However, the derivation below is valid for any set $\mathcal{N}$ with $|\mathcal{N}| = N$.

Following a derivation analogous to that in Section 2, we use Lagrange optimization with the additional finite length constraint. The minimization produces $N+1$ linear equations,

$$\sum_{n\in\mathcal{N}} c[n]\phi_{hh}((k-n)T) = 0, \quad k \neq 0 \tag{38}$$
$$\sum_{n\in\mathcal{N}} c[n]\phi_{hh}(-nT) + \frac{\lambda}{2} = 0, \quad k = 0 \tag{39}$$
$$c[0] + x[0] = 0 \tag{40}$$

As shown in Section 3, the second-derivatives are all positive, thus equations (38), (39), (40) have a unique solution corresponding to the optimal compensation signal for the given value of N. We express these equations in block matrix form,

$$\begin{bmatrix} \phi_{\mathbf{hh}} & \frac{1}{2}\delta \\ \delta^{\mathbf{T}} & 0 \end{bmatrix} \begin{bmatrix} \mathbf{c_n} \\ \lambda \end{bmatrix} = \begin{bmatrix} \mathbf{0} \\ -x[0] \end{bmatrix} \tag{41}$$

where λ is the Lagrange multiplier, δ is a vector with all zero entries except for a 1 as the center element, and $\mathbf{c_n}$ is a vector representation of $c[n]$. $\phi_{\mathbf{hh}}$ is a Toeplitz, symmetric matrix containing N samples of $\phi_{hh}(\tau)$, the autocorrelation of $h(t)$.

$$\phi_{\mathbf{hh}}(i,j) = \phi_{hh}((i-j)T), \quad |i-j| \in \mathcal{N} \tag{42}$$

For certain degenerate interpolation filters, $\phi_{\mathbf{hh}}$ may be singular. We do not consider such cases. Assuming $\phi_{\mathbf{hh}}$ is invertible, the block matrix (41) can be solved for the Lagrange multiplier and optimal finite-length compensation signal, $c_{\text{ofax}}[n]$.

$$\lambda = \frac{2x[0]}{\kappa} \tag{43}$$
$$c_{\text{ofax}}[n] = -\frac{x[0]}{\kappa}\phi_{\mathbf{hh}}^{-\mathbf{1}}\delta \tag{44}$$

where $\kappa = \delta^{\mathbf{T}}\phi_{\mathbf{hh}}^{-1}\delta$. We refer to the algorithm represented by (46) as Optimal Finite Approximation (OFAX). There are efficient numerical techniques for computing $c_{\text{ofax}}[n]$ that exploit the Toeplitz, symmetric structure of $\phi_{\mathbf{hh}}$. In any case, the computation only needs to be done once, since once $c[n]$ is determined it can be stored and retrieved when the algorithm

needs to be applied. This is the case with all of the finite-length approximations explored, OFAX, DPAX, and IA.

The development above is general for any form of the interpolation filter $h(t)$. In the remaining part of this section, we focus our analysis on the case that $h(t)$ is an oversampled, sinc-interpolating filter and the time-axis is normalized such that $T = 1$. As shown in Section 4, the problem can be posed directly in DT when $h(t)$ is band-limited. In this case, $h[n]$ is a DT sinc-interpolating filter with cutoff γ. We denote its autocorrelation matrix using $\mathbf{\Theta}_\gamma$, reserving $\phi_{\mathbf{hh}}$ for the general case. Using frequency domain arguments, it is straightforward to show that,

$$\mathbf{\Theta}_\gamma(i,j) = \mathrm{sinc}(\gamma(i-j)) \tag{45}$$

From [2] we know $\mathbf{\Theta}_\gamma$ is invertible. In this case, the OFAX solution is,

$$c_{\mathrm{ofax}}[n] = -\frac{x[0]}{\kappa}\mathbf{\Theta}_\gamma^{-\mathbf{1}}\delta \tag{46}$$

where $\kappa = \delta^{\mathbf{T}}\mathbf{\Theta}_\gamma^{-\mathbf{1}}\delta$.

The OFAX algorithm was implemented for oversampled, sinc-interpolating filters in MATLAB and examples of $c_{\mathrm{ofax}}[n]$ were computed in which $x[0] = -1$. Figure 1(a) illustrates $c_{\mathrm{ofax}}[n]$ and $|C_{\mathrm{ofax}}(e^{j\omega})|$, the magnitude of a 2048-point zero-padded discrete Fourier transform (DFT), for various values of N and $\gamma = 0.9\pi$. Figure 1(b) illustrates the same for $\gamma = 0.7\pi$. As expected, $c_{\mathrm{ofax}}[n]$ is high-pass with the main-lobe of the DFT centered at $\omega = \pi$, and smaller energy side-lobes at lower frequencies. As N increases, the energy in the pass-band $[-\gamma, \gamma]$ decreases, thus decreasing the error, $\mathcal{E}^2$. Furthermore, for the same N, the solution for $\gamma = 0.7\pi$ performs better than that for $\gamma = 0.9\pi$ because there is a larger guard-band. Intuitively, the system is more oversampled, and there is greater redundancy, so a better solution can be found using fewer points.

Figure 2(a) illustrates $\mathcal{E}^2$ as a function of N. The graph shows that $\mathcal{E}^2$ decreases approximately exponentially in N. Since the OFAX algorithm generates the optimal solution, the error curves shown in Figure 2(a) serve as a baseline for performance of other finite-length choices for $c[n]$.

In this case, where $h(t)$ is an ideal, sinc-interpolating filter, the solution becomes numerically unstable to the precision of MATLAB, beyond $\mathcal{E}^2 = 10^{-9}$. In practical systems, though the interpolation filter is never ideal. In general, non-ideal $h(t)$ impose looser restrictions, making the OFAX solution better conditioned and computable to lower error values. Also, in either case, the error can be made arbitrarily low by performing the computation on a computer with arbitrarily high precision. $\mathcal{E}^2 = 10^{-9}$ is thus a worst-case bound on minimum achievable error. Even then, in most contexts, an error of $10^{-9} = -180$dB, compared to the signal, is more than sufficient.

As in Section 3, generalization to multiple erasures requires constrained minimization with multiple constraints. The development is analogous to that above, except there are multiple Lagrange multiplier terms, one for each erasure. In addition, $\mathcal{N}$ will likely be non-sequential, with a group of points around each erasure. Though rigorous, globally minimizing the OFAX solution using every erasure is unnecessary in most cases. If erasures are widely spaced, a reasonable result can be achieved by superimposing single-erasure OFAX solutions.

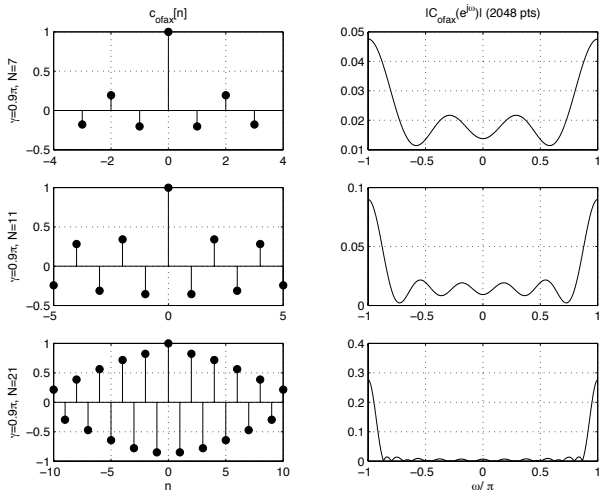

(a) $\gamma = 0.9\pi$

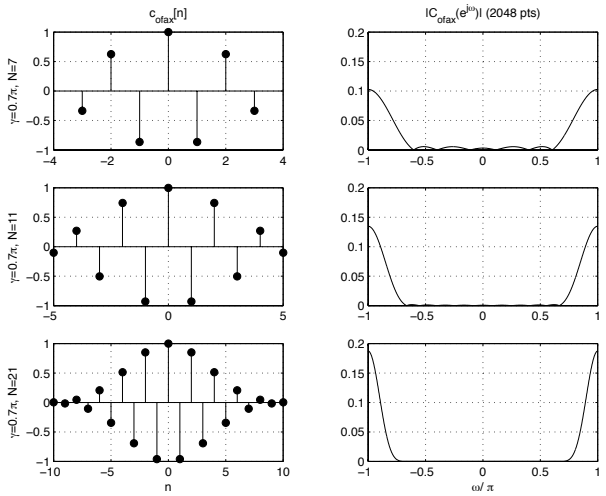

(b) $\gamma = 0.7\pi$

Fig. 1. Optimal finite-length compensation sequences, $c_{\mathrm{ofax}}[n]$, for oversampled, sinc-interpolating filters computed using OFAX. The plots for two different cutoffs, $\gamma = 0.7\pi$ and 0.9π, and N =7, 11, 21 are on the left. The 2048-point zero-padded Fourier Transform of each of these sequences is on the right. The transforms are linearly interpolated for display.

VI. Discrete Prolate Approximation

In this section, we develop another finite-length solution that is an approximation to the optimal, finite-length solution for oversampled, sinc-interpolating filters. With OFAX, we construct a finite-length compensation signal directly from the imposed constraints. Alternatively, for the case of oversampled, sinc-interpolating filters, we can start with the unconstrained solution, $c_{\mathrm{ideal}}[n] = -x[0](-1)^n$, and truncate it through appropriate windowing. In this case, we apply a finite-length

window, $w[n]$, such that

$$c[n] = w[n]c_{\text{ideal}}[n] \tag{47}$$

has minimum energy in the frequency band $|\omega| < \gamma$. As in Section 4, we restrict $c[n]$ to the set $\mathcal{N} = [-\frac{N-1}{2}, \frac{N-1}{2}]$. Note that since $c_{\text{ideal}}[n] = -x[0](-1)^n$, $C(e^{j\omega})$ is the Fourier transform of the window centered around π. Consequently, as per (31) our goal is to design $w[n]$ that has finite-support $[-\frac{N-1}{2}, \frac{N-1}{2}]$, meets the constraint $w[0] = 1$, and maximizes the energy in the band $|\omega| < \pi - \gamma$.

Slepian, Landau, and Pollak solved this problem in [2] through the development of discrete prolate spheroidal sequences (DPSS). Using variational methods it is shown in [2] that, normalized by total energy, the signal $w[n]$ that maximizes the energy in the band $\omega < \Omega$ is an eigenvector of an $N \times N$ symmetric, positive-definite, Toeplitz matrix, $\mathbf{\Theta_\Omega}$, with elements

$$\mathbf{\Theta_\Omega}[n, m] = \text{sinc}(\Omega(m - n)) \tag{48}$$

$$m, n = -\frac{N-1}{2}, ... - 1, 0, 1, ...\frac{N-1}{2}$$

By the spectral theorem, the eigenvectors, $v_i^\Omega[n]$, are real and orthogonal with associated real, positive eigenvalues, λ_i^Ω. In addition, these particular eigenvalues are always distinct. The eigenvectors, $v_i^\Omega[n]$, are the discrete prolate spheroidal sequences (DPSS) for the bandwidth Ω and length N. They form a finite orthonormal basis for the space of finite-energy signals time-limited to $[-\frac{N-1}{2}, \frac{N-1}{2}]$, [2].

The eigenvalues represent the proportion of total energy in the band $\omega < \Omega$, [2]. Consequently, the first eigenvector, $v_1^\Omega[n]$, is the solution to the maximum energy problem. In our particular case, $\Omega = \pi - \gamma$, and after scaling to meet the constraint $w[0] = 1$, the optimal window is

$$w[n] = \frac{1}{v_1^{\pi-\gamma}[0]} v_1^{\pi-\gamma}[n] \tag{49}$$

Multiplying the window with $c_{\text{ideal}}[n]$ results in a potential compensation signal

$$c_{\text{dpax}}[n] = -\frac{x[0]}{v_1^{\pi-\gamma}[0]}(-1)^n v_1^{\pi-\gamma}[n] \tag{50}$$

As stated in [2], every DPSS has a dual symmetric partner. In particular,

$$v_{N+1-i}^\Omega[n] = (-1)^n v_i^{\pi-\Omega}[n] \tag{51}$$

The eigenvalues are related,

$$\lambda_{N+1-i}^\Omega = \lambda_i^{\pi-\Omega} \tag{52}$$

In addition, it is straightforward to infer from [2] that the eigenvalues of the same band-width are related,

$$\lambda_i^\Omega = 1 - \lambda_{N+1-i}^\Omega \tag{53}$$

Duality implies that the compensation signal, $c_{\text{dpax}}[n]$ in (50), can be equivalently expressed as,

$$c_{\text{dpax}}[n] = -\frac{x[0]}{v_N^\gamma[0]} v_N^\gamma[n] \tag{54}$$

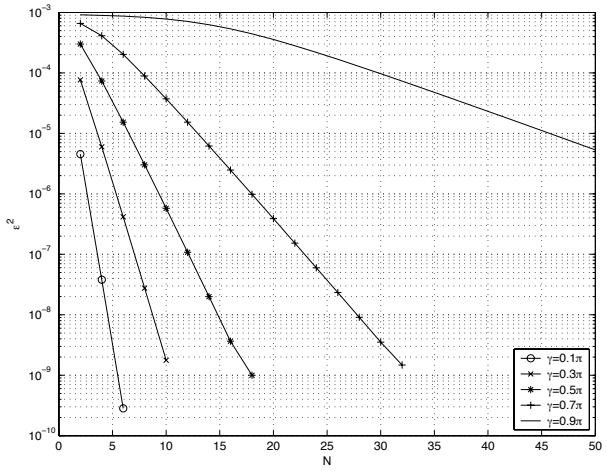

(a) $\mathcal{E}^2_{\text{ofax}}$, the squared-error of c_{ofax}

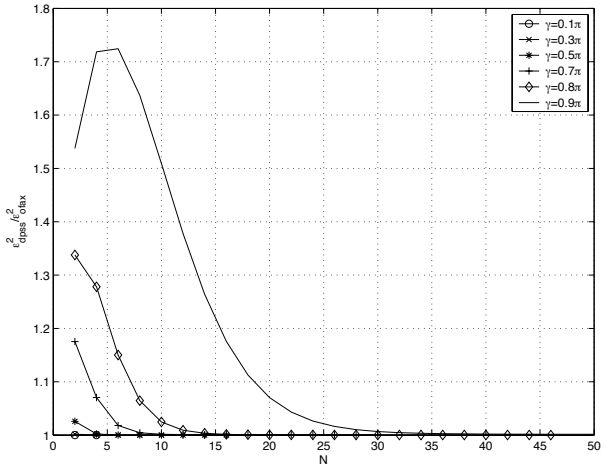

(b) Comparative error ratio $\mathcal{E}^2_{\text{dpax}}/\mathcal{E}^2_{\text{ofax}}$

Fig. 2. Error performance of OFAX and DPAX as a function of N. Upper plot illustrates the squared-error of optimal OFAX compensation for oversampled, sinc-interpolating filters with cutoffs $\gamma = 0.1\pi, 0.3\pi, 0.5\pi, 0.7\pi, 0.9\pi$. Lower plot illustrates the increase in error due to using DPAX, rather than the optimal OFAX solution, in the case of oversampled, sinc-interpolating with cutoffs $\gamma = 0.1\pi, 0.3\pi, 0.5\pi, 0.7\pi, 0.8\pi, 0.9\pi$.

Where $v_N^\gamma[n]$ is the last eigenvector of the matrix $\mathbf{\Theta}_\gamma$. Independent of which DPSS is used to express it, we denote this solution as the Discrete Prolate Approximation (DPAX). For asymmetric compensation not centered around the erasure, the solution is the same, except that the scaling is relative to the erasure, $v_N^\gamma[k]$, for $k \neq 0$.

It should be clear that $c_{\text{dpax}}[n]$ is not equivalent to the ideal low-pass OFAX solution, $c_{\text{ofax}}[n]$. The window formulation starts with a finite-energy signal, optimizes for that energy, and then scales to meet the $c[0] = -x[0]$ constraint. OFAX does not begin with an energy constraint; therefore it finds the optimal solution. The exact relationship between $c_{\text{dpax}}[n]$ and $c_{\text{ofax}}[n]$ can be found by decomposing $c_{\text{ofax}}[n]$ in the DPSS basis, $\{v_i^\gamma[n]\}$. The DPSS form the orthonormal eigenvector

basis that diagonalizes $\mathbf{\Theta}_\gamma$,

$$\mathbf{\Theta}_\gamma = \mathbf{V}\mathbf{\Lambda}\mathbf{V}^\mathbf{T} \tag{55}$$

where the columns of $\mathbf{V}$ are the DPSS $v_i^\gamma[n]$, and $\mathbf{\Lambda}$ is a diagonal matrix of the eigenvalues λ_i^γ. It follows from [2] that $\mathbf{\Theta}_\gamma$ is invertible and that $c_{\mathrm{ofax}}[n]$ exists. Furthermore, $c_{\mathrm{ofax}}[n]$ can thus be expressed as

$$c_{\mathrm{ofax}}[n] = -\frac{x[0]}{\kappa}\left(\frac{1}{\lambda_1^\gamma}\beta_1 v_1^\gamma[n] + \cdots + \frac{1}{\lambda_N^\gamma}\beta_N v_N^\gamma[n]\right) \tag{56}$$

where $\beta_i = v_i^\gamma[0]$, $\kappa = \delta^\mathbf{T}\mathbf{\Theta}_\gamma^{-\mathbf{1}}\delta = \sum_{i=1}^N \frac{1}{\lambda_i^\gamma}(v_i^\gamma[0])^2$, and the eigenvalues are distributed between 0 and 1. The expression for the optimal solution depends on the reciprocals $1/\lambda_i^\gamma$, so the eigenvector with the smallest eigenvalue, $v_N^\gamma[n]$, will dominate. Since scaling this vector produces $c_{\mathrm{dpax}}[n]$, DPAX can be interpreted as a first-order approximation to $c_{\mathrm{ofax}}[n]$.

Figure 2(b) shows the comparative error ratio, $\mathcal{E}^2_{\mathrm{dpax}}/\mathcal{E}^2_{\mathrm{ofax}}$, due to DPAX. The increase in error becomes negligible as N increases and γ decreases. Additionally, DPAX does not suffer from the same ill-conditioning problems as the ideal low-pass OFAX solution, so, by increasing N, it can achieve values of $\mathcal{E}^2$ near 10^{-20} in MATLAB, i.e. about ten orders of magnitude smaller than that using OFAX.

The near-optimal performance of the DPAX solution is explained by the eigenvalue distribution of $\mathbf{\Theta}_\gamma$. As N increases and γ decreases, the reciprocal of the smallest eigenvalue, $1/\lambda_N$, increasingly dominates the reciprocals of the other eigenvalues. In (56), $v_N^\gamma[n]$ dominates the other terms, making $c_{\mathrm{dpax}}[n]$ a tighter approximation.

The DPAX solution can be computed directly as the last eigenvector of $\mathbf{\Theta}_\gamma$ or the first eigenvector of $\mathbf{\Theta}_{\pi-\gamma}$. This computation is often degenerate because the eigenvalues of $\mathbf{\Theta}_\gamma$ are clustered around 0 or 1. Fortunately, there exist standard techniques around this problem that involve replacing $\mathbf{\Theta}_\gamma$ with a symmetric, tri-diagonal matrix which has eigenvalues that are well spread, [2], [3].

The DPAX algorithm was implemented in MATLAB and examples of $c_{\mathrm{dpax}}[n]$ were computed in which $x[0] = -1$. The DPSS were found using the `dpss` function in the Signal Processing Toolbox. Figure 3(a) shows $c_{\mathrm{dpax}}[n]$ and $|C_{\mathrm{dpax}}(e^{j\omega})|$, the magnitude of a 2048-point zero-padded DFT, for various values of N and $\gamma = 0.9\pi$. Figure 3(b) shows the same for $\gamma = 0.7\pi$. $c_{\mathrm{dpax}}[n]$ looks similar to $c_{\mathrm{ofax}}[n]$, except for the outlying zeroth sample in $c_{\mathrm{ofax}}[n]$. Also, like $c_{\mathrm{ofax}}[n]$, $c_{\mathrm{dpax}}[n]$ performs better when γ is smaller and there is a larger guard-band.

DPAX can be extended to multiple erasures by superimposing single-erasure DPAX solutions. DPAX is a purely local strategy, i.e. $c_{\mathrm{dpax}}[n]$ is completely specified by the erasure, $x[i]$, and the length N of the compensation. In contrast, OFAX is a global strategy, so we can potentially do better than simple superposition if we choose to do the minimization using multiple constraints.

In any case, DPAX is a powerful alternative algorithm to OFAX. It is simpler to implement and it decouples the design of $c[n]$ from the exact form of the interpolation filter. Furthermore, as long as $h(t)$ is sufficiently low-pass, DPAX should perform reasonably well for the the entire class of filters that have cutoff at approximately γ.

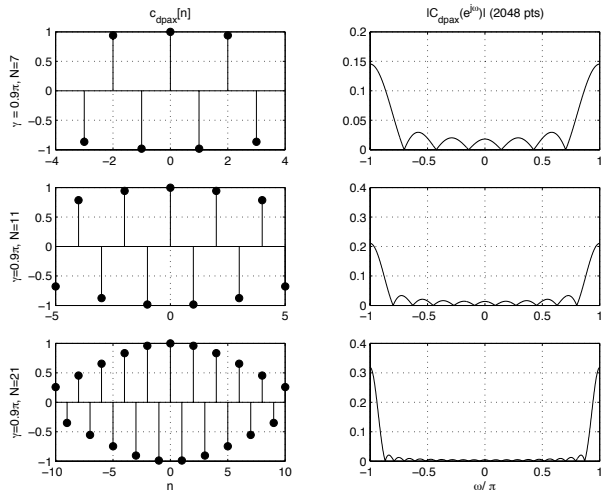

(a) $\gamma = 0.9\pi$

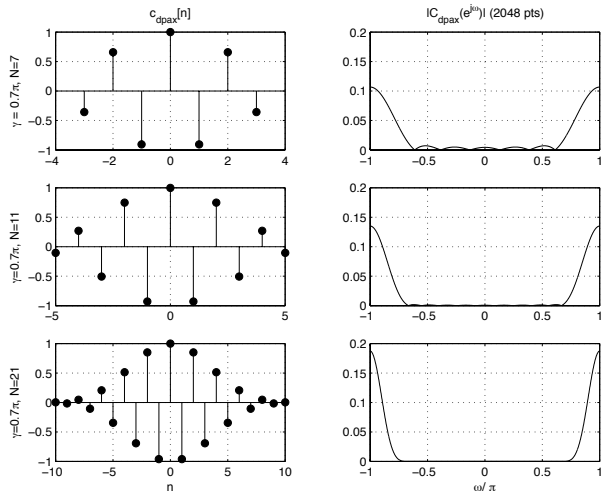

(b) $\gamma = 0.7\pi$

Fig. 3. DPAX solution, $c_{\mathrm{dpax}}[n]$, for two different cutoffs, $\gamma = 0.7\pi$ and 0.9π, and N =7, 11, 21 are on the left. The 2048-point zero-padded Fourier Transform of each of these sequences is on the right. The transforms are linearly interpolated for display.

VII. Iterative Approximation

In this section, as an alternative to the two closed-form algorithms for finite length approximation, we develop an iterative solution in the class of projection-onto-convex sets (POCS). As with DPAX, the algorithm developed is specific to the the case of oversampled, sinc-interpolating filters.

Figure 4(a) is a block diagram of the algorithm, denoted Iterative Approximation (IA). We constrain the initial input $\mathbf{w}^{(0)}$ to be in ℓ_2, the class of finite-energy DT signals. Each iteration then consists of three sequential projections, P_B onto the subspace of ℓ_2 band-limited to $\pi - \gamma$, $P_\mathcal{N}$ onto the

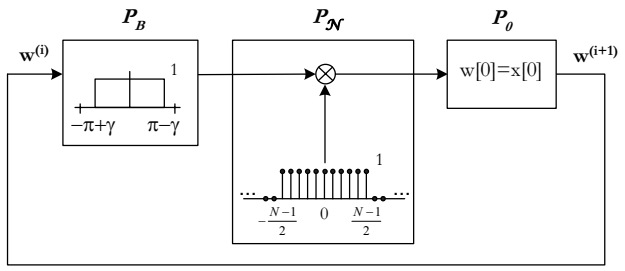

(a) POCS Iteration

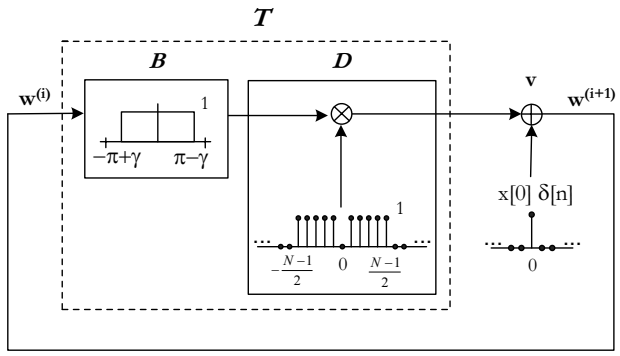

(b) Affine Iteration

Fig. 4. Block diagrams for IA algorithm. (a) illustrates POCS implementation with three iterated projections $P_B, P_{\mathcal{N}}$, and P_0. (b) illustrates equivalent affine implementation with linear operators $B = P_B$ and D which are combined into the composite linear operator T. The initial input, $\mathbf{w^{(0)}}$, is constrained to ℓ_2.

subspace of ℓ_2 time-limited to $[-\frac{N-1}{2}, \frac{N-1}{2}]$, and P_0 onto the hyper-plane defined by the constraint $c[0] = -x[0]$. Note that in Figure 4 we have changed to a vector notation for the signals. In particular, $\mathbf{w}^{(i)}$ represents the signal $w[n]$ at the i-th iteration.

The iteration can be proved to converge uniquely to $(-1)^n c_{\text{ofax}}[n]$. To facilitate certain proofs, we represent the projections in Figure 4(a) in terms of the affine transformation of Figure 4(b). The two representations are isomorphic, i.e. they result in the same solution after each iteration. In the affine representation, there are three steps in each iteration. The first step is $B = P_B$, a band-limiting operator, i.e. an ideal low-pass filter with cut-off $\pi - \gamma$. The second step is D, a truncation operator that time-limits to $[-\frac{N-1}{2}, \frac{N-1}{2}]$ and additionally removes the value at index $n = 0$. B and D can be combined into one linear operator T. The last step in the iteration is the addition of an impulse, denoted in the vector notation as $\mathbf{v} = x[0]\delta[n]$.

We begin by proving the existence of a fixed point. We do this directly, by substituting $(-1)^n c_{\text{ofax}}[n]$ into the POCS iteration. In Figure 4(a), P_B and $P_{\mathcal{N}}$ define a time-limited convolution. It is straightforward to show that this operation can be expressed in matrix form as $\mathbf{\Theta}_{\pi-\gamma}$, the Toeplitz matrix in equation (48) with $\Omega = \pi - \gamma$. Using the decomposition of $c_{\text{ofax}}[n]$, as per (56),

$$P_0 P_B P_{\mathcal{N}} \{(-1)^n c_{\text{ofax}}[n]\} = P_0 \left\{ \frac{-x[0]}{\kappa} \mathbf{\Theta}_{\pi-\gamma} \left(\frac{\beta_1}{\lambda_1^\gamma}(-1)^n v_1^\gamma[n] + \cdots + \frac{\beta_N}{\lambda_N^\gamma}(-1)^n v_N^\gamma[n] \right) \right\} \quad (57)$$

Applying the dual symmetry of the DPSS and substituting (51) into (57),

$$P_0 P_B P_{\mathcal{N}} \{(-1)^n c_{\text{ofax}}[n]\} = P_0 \left\{ \frac{-x[0]}{\kappa} \left(\frac{\beta_1}{\lambda_1^\gamma} \mathbf{\Theta}_{\pi-\gamma} v_N^{\pi-\gamma}[n] + \cdots + \frac{\beta_N}{\lambda_N^\gamma} \mathbf{\Theta}_{\pi-\gamma} v_1^{\pi-\gamma}[n] \right) \right\} \quad (58)$$

Applying the eigenvector identity and substituting $\lambda_i^{\pi-\gamma} = 1 - \lambda_{N+1-i}^\gamma$ as per (52) and (53),

$$P_0 P_B P_{\mathcal{N}} \{(-1)^n c_{\text{ofax}}[n]\} = P_0 \left\{ \frac{-x[0]}{\kappa} \left(\frac{\beta_1(1-\lambda_1^\gamma)}{\lambda_1^\gamma} v_1^{\pi-\gamma}[n] + \cdots + \frac{\beta_N(1-\lambda_N^\gamma)}{\lambda_N^\gamma} v_N^{\pi-\gamma}[n] \right) \right\} \quad (59)$$

Reapplying the dual symmetry of the DPSS and substituting (51) into (59), the equation can be manipulated into two terms, one that is $(-1)^n c_{\text{ofax}}[n]$ and the other, which is composed of residual terms without factors of λ_i^γ.

$$P_0 P_B P_{\mathcal{N}} \{(-1)^n c_{\text{ofax}}[n]\} = P_0 \left\{ (-1)^n c_{\text{ofax}}[n] - \frac{-x[0]}{\kappa}(-1)^n \left(\beta_1 v_1^\gamma[n] + \cdots + \beta_N v_N^\gamma[n] \right) \right\} \quad (60)$$

Recalling that $\beta_i = v_i^\gamma[0]$, we observe that the residual terms form the decomposition of a scaled impulse in the orthonormal DPSS basis $\{v_i^\gamma[n]\}$,

$$\beta_1 v_1^\gamma[n] + \cdots + \beta_N v_N^\gamma[n] = \underbrace{\langle v_1^\gamma[n], \delta[n] \rangle}_{v_1^\gamma[0]} v_1^\gamma[n] + \cdots + \underbrace{\langle v_N^\gamma[n], \delta[n] \rangle}_{v_N^\gamma[0]} v_N^\gamma[n] = \delta[n] \quad (61)$$

Projection with P_0 removes the scaled impulse and returns $(-1)^n c_{\text{ofax}}[n]$.

$$P_0 P_B P_{\mathcal{N}} \{(-1)^n c_{\text{ofax}}[n]\} = P_0 \left\{ (-1)^n c_{\text{ofax}}[n] - \frac{-x[0]}{\kappa}\delta[n] \right\} = (-1)^n c_{\text{ofax}}[n] \quad (62)$$

This proves the existence of a fixed point. We next show convergence using the affine representation of Figure 4(b).

Assuming that $\mathbf{w}^{(0)}$ is in ℓ_2, the iteration defines a sequence in ℓ_2,

$$\mathbf{w}^{(n+1)} = T\mathbf{w}^{(n)} + \mathbf{v} \tag{63}$$

We define the error signal after each iteration, $\mathbf{e}^{(i)} = \mathbf{w}^{(i)} - \mathbf{w}^*$. Applying T to both sides, adding $\mathbf{v}$, and rearranging the expression we conclude that,

$$\mathbf{e}^{(i+1)} = T\mathbf{e}^{(i)} \tag{64}$$

Convergence implies that the energy of $\mathbf{e}^{(i)}$, denoted in norm-notation as $\|\mathbf{e}^{(i)}\|_2$, approaches zero as i goes to infinity. Thus, a sufficient condition for convergence is that T is a strictly non-expansive operator, i.e. for $\mathbf{w_1} \neq \mathbf{w_2}$, $\|T(\mathbf{w_1} - \mathbf{w_2})\|_2 < \|\mathbf{w_1} - \mathbf{w_2}\|_2$. In our case, T has two components: band-limiting, B, and truncation, D. The input to B, $\mathbf{w}^{(i)}$, is a signal time-limited to $[-\frac{N-1}{2}, \frac{N-1}{2}]$ that has $w[0] > 0$. Aside from the zero-signal, the set of band-limited signals and set of time-limited signals are disjoint. $\mathbf{w}^{(i)}$ is not the zero-signal, so by Parseval's theorem B strictly reduces the energy in the input $\mathbf{w}^{(i)}$. The output, $B\mathbf{w}^{(i)}$, is band-limited. Invoking the fact that the set of band-limited and time-limited signals are disjoint again, we can assert that D strictly reduces the energy of $B\mathbf{w}^{(i)}$ and thus,

$$\|T\mathbf{w}^{(i)}\|_2 < \|\mathbf{w}^{(i)}\|_2 \tag{65}$$

This inequality fails only when $\mathbf{w} = \mathbf{0}$. In other words, $\|T(\mathbf{w_1} - \mathbf{w_2})\|_2 < \|(\mathbf{w_1} - \mathbf{w_2})\|_2$ unless $\mathbf{w_1} = \mathbf{w_2}$. Thus, T is a strictly-non-expansive operator and IA converges strongly to some set of fixed points.

In fact, a strictly non-expansive T implies that IA converges strongly to a unique fixed-point. This follows by contradiction. Suppose that there are two fixed-points, $\mathbf{w_1^*}$ and $\mathbf{w_2^*}$, that are linearly independent such that $\mathbf{w_2^*} \neq \beta\mathbf{w_1^*}$, for any $\beta \in \Re$. Since they are both fixed-points,

$$T\mathbf{w_1^*} + \mathbf{v} = \mathbf{w_1^*} \tag{66}$$

$$T\mathbf{w_2^*} + \mathbf{v} = \mathbf{w_2^*} \tag{67}$$

Subtracting the two expressions and using the linearity of T, implies

$$T(\mathbf{w_1^*} - \mathbf{w_2^*}) = \mathbf{w_1^*} - \mathbf{w_2^*} \tag{68}$$

Since we know that T is a strictly non-expansive operator, this implies that $\mathbf{w_1^*} = \mathbf{w_2^*}$, a contradiction. Thus $\mathbf{w}^* = (-1)^n c_{\text{ofax}}[n]$ is the unique fixed-point.

Although IA converges to the optimal solution, numerical simulation shows that, as N increases and γ decreases, the convergence rate slows to the point of making IA impractical compared to OFAX. Figure 5 illustrates the convergence curves for various N and γ. Slow convergence is caused by the fact that the eigenvalues of $\mathbf{\Theta}_{\pi-\gamma}$ are clustered near 1, so there is minimal change between iterations. Though not studied in this treatment, POCS relaxation techniques could potentially be used to speed up the convergence rate.

Extending IA for multiple erasures requires us to replace multiple samples in the P_0 step, rather than just one. For this more general case, we conjecture that the iteration will converge to the multiple erasure OFAX solution found using minimization with multiple constraints.

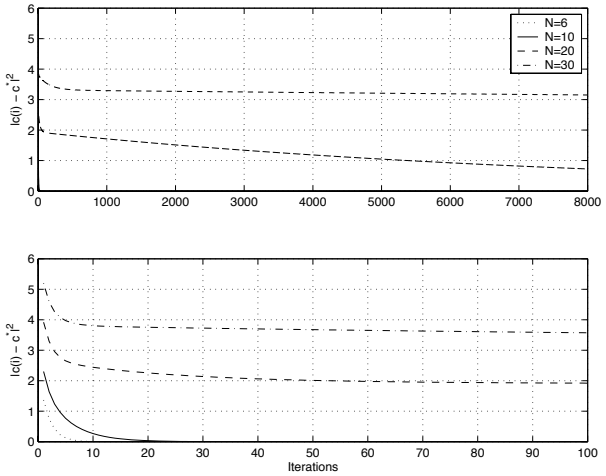

(a) Convergence curves for $\gamma = 0.7\pi$

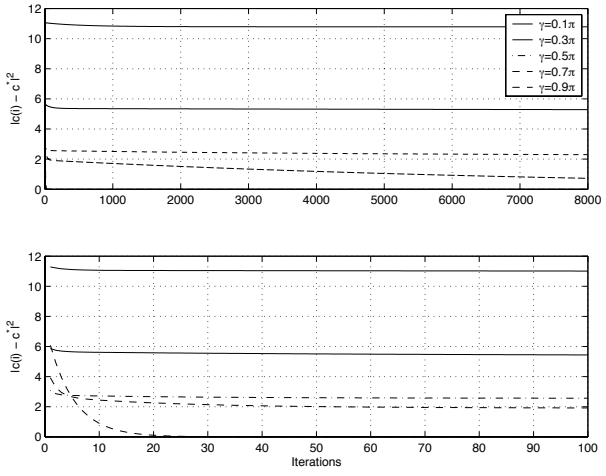

(b) Convergence curves for $N = 20$

Fig. 5. Convergence of IA algorithm for oversampled, sinc-interpolating filters. (a) illustrates the squared-distance of $\mathbf{w^{(i)}}$ from the fixed point, $\mathbf{w}^*$, for $\gamma = 0.7\pi$ and $N = 6, 10, 20, 30$. The initial input is $\mathbf{w^{(0)}} = \mathbf{0}$. The upper plot shows the result out to 8000 iterations. The lower plot shows an inset, out to 100 iterations. (b) illustrates the same for $N = 20$ and $\gamma = 0.1\pi, 0.3\pi, 0.5\pi, 0.7\pi, 0.9\pi$.

VIII. Potential Application: Compensating Displays with Missing Pixels

In flat-panel displays some picture elements (pixels) can become defective with the result that they are permanently black. This represents an example of the type of erasure considered in this paper. Some solutions to compensating for faulty pixels in these displays have been proposed previously [4], [5]. The patents are based on brightening neighboring pixels in order to compensate for the permanently dark pixels.

The one-dimensional solutions presented in this paper can potentially be applied to the two-dimensional displays on a row-by-row and column-by-column basis. In future work, the theoretical framework developed in this paper can also be

extended to multiple dimensions although those extensions do not appear to be straight forward. As an informal and very preliminary illustration, we applied a two-dimensional version of the OFAX algorithm to the image in Figure 6(a), with the result shown in Figure 6(b). Because of the informality of the example, this should be viewed simply as a visual illustration of how the compensation works, rather than a practical validation of the theory.

In this example, 5% of the pixels have been randomly chosen as defective, i.e. permanently set to black. The upper image represents a display with defective pixel elements. The lower plot shows the result when OFAX along the lines of Section 4 has been used to adjust values of a 5×5 region of neighboring pixels, centered on the missing pixel. Thus, for each missing pixel, $N = 24$ surrounding pixels are adjusted. The compensation is done independently for each defective pixel.

We use a 2-D version of the OFAX equations, m is along the y-axis, and $\mathcal{M} = [-2, 2]$ and n is along the x-axis with $\mathcal{N} = [-2, 2]$. The full set of equations are of the form,

$$\sum_{m\in\mathcal{M}}\sum_{n\in\mathcal{N}} c[m,n]\phi_{hh}(k_1-m,k_2-n) = 0, \qquad (69)$$

$$k_1 \neq \text{ or } k_2 \neq 0$$

$$\sum_{m\in\mathcal{M}}\sum_{n\in\mathcal{N}} c[m,n]\phi_{hh}(-m,-n) + \frac{\lambda}{2} = 0, \qquad (70)$$

$$k_1 = 0 \text{ and } k_2 = 0$$

$$c[0,0] + x[0,0] = 0 \qquad (71)$$

We assume that the spatial frequency response of the eye for each color, red, green, blue, is modeled as a radially symmetric decaying exponential [6],

$$H_{eye}(\omega_1,\omega_2) = e^{-\alpha\sqrt{\omega_1^2+\omega_2^2}} \qquad (72)$$

where α is a constant that defines the amount of blurring dependent on the distance we view picture from. In our example, we set α according to [6] such that the viewing distance is 5 feet (1.524 meters). After computation, the sequence $c[n, m]$ was scaled and added to the image for each color, red, green, blue, at the different defective pixel locations. We do not address the amplitude-limited nature of the display and allow the compensation to clip. Empirically, it seems that clipping occurs rarely for this particular image. Though the compensation is informal, there appears to be a significant improvement in perceived image quality.

ACKNOWLEDGMENT

This work was supported in part by the Paul and Daisy Fellowship for New Americans and the Texas Instruments DSPS Leadership University Program. The work was also prepared through collaborative participation in the Advance Sensors Collaborative Technology Alliance (CTA) sponsored by the U.S. Army Research Laboratory under Cooperative Agreement DAAD19-01-2-008. The authors would also like to thank our three anonymous reviewers for their excellent suggestions and comments. The authors would also like to thank their colleague, Petros Boufounos, for first suggesting the application of erasure compensation to flat-panel displays.

REFERENCES

[1] A. V. Oppenheim, R. W. Schafer, and J. R. Buck, *Discrete-Time Signal Processing*. Prentice Hall, 1999.
[2] D. Slepian, "Prolate Spheroidal Wave Functions, Fourier Analysis, and Uncertainty –V: The Discrete Case," *Bell System Technical Journal*, 1978.
[3] T. Verma, S. Bilbao, and T. H. Y. Meng, "The Digital Prolate Spheroidal Window," in *1996 IEEE ICASSP Conference Proceedings*, 1996.
[4] V. Markandey, R. J. Gove, and T. I. Inc., "Method of reducing the visual impact of defects present in a spatial light modulator display," U.S. Patent 5,504,504, 1996.
[5] R. G. Fielding and R. B. Ltd., "Video display systems," International Patent WO 91/15843, 1991.
[6] R. Näsänen, "Visibility of halftone dot textures," *IEEE Transactions on Systems, Man, and Cybernetics*, vol. 14, pp. 920–924, Nov. 1984.

PLACE PHOTO HERE

Sourav R. Dey Sourav R. Dey (S'04) received the S.B degrees in electrical engineering and mathematics from the Massachusetts Institute of Technology (MIT) in 2002 and 2003, respectively. He received his M.Eng degree in electrical engineering in 2004 from MIT. He is currently working toward his Ph.D in the Digital Signal Processing Group under the supervision of Prof. Oppenheim. Current research interests include data-dependent sampling, noise-shaping, and statistical inference.

Sourav is a member of Tau Beta Pi and Eta Kappa Nu. He is a recipient of both the Paul and Daisy Soros Fellowship for New Americans and the National Defense Science and Engineering Graduate (NDSEG) Fellowship. He is also a recipient of the 2004 Ernst. A Guillemin Thesis Award for outstanding M.Eng thesis and the 2002 George C. Newton Award for outstanding undergraduate project from the Department of Electrical Engineering and Computer Science at MIT.

PLACE PHOTO HERE

Andrew I. Russell Andrew I. Russell (S'01-M'03) was born in Kingston, Jamaica, in 1975. He received the S.B., M.Eng. and Ph.D. degrees from the Department of Electrical Engineering and Computer Science, Massachusetts Institute of Technology (MIT), in 1998, 1999 and 2002 respectively. While at MIT. Dr. Russell was with the Digital Signal Processing Group, Research Laboratory of Electronics.

Since 2003, Dr. Russell has been a lecturer in the Department of Physics at the University of the West Indies (UWI), in Jamaica. He has taught classes on DSP and introductory electronics. While at UWI, Dr. Russell has also been doing algorithm development for Texas Instruments Inc., Plano, Texas. He has also worked for Bose Corporation, Framingham, Massachusetts, and Vanu Inc., Cambridge, Massachusetts. His research interests include filter design, sampling rate conversion, nonuniform sampling, nonlinear signal processing and image processing.

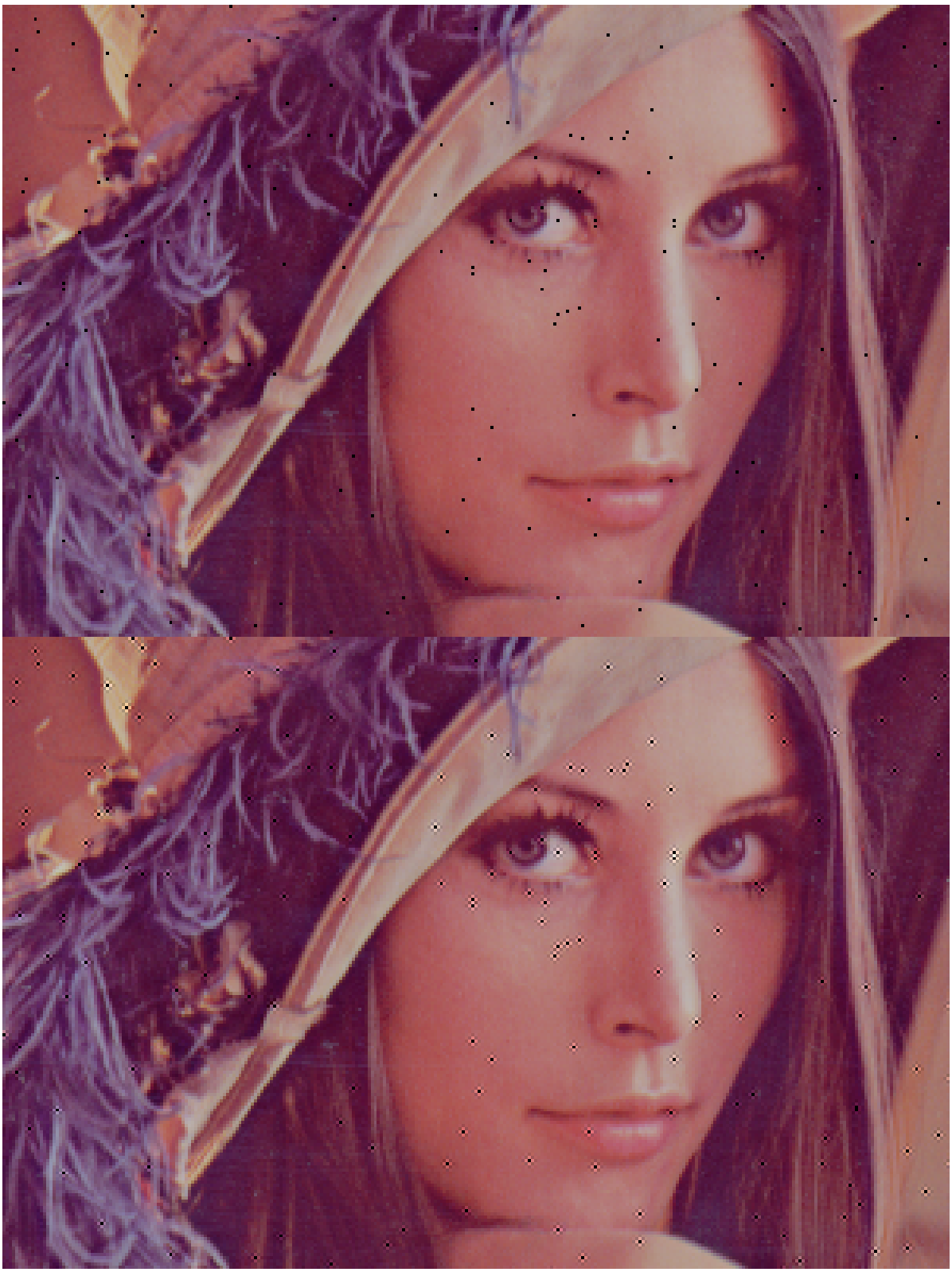

Fig. 6. Simulated video display with defective pixels. Upper image illustrates uncorrected image. Lower image illustrates the same image with a 5×5 grid of pixels ($N = 24$) around each missing pixel modified using the OFAX algorithm with the interpolation filter (72). A viewing distance of 5 feet (1.524 meters) is recommended

PLACE
PHOTO
HERE

Alan V. Oppenheim Alan V. Oppenheim received the S.B. and S.M. degrees in 1961 and the Sc.D. degree in 1964, all in electrical engineering, from the Massachusetts Institute of Technology. He is also the recipient of an honorary doctorate from Tel Aviv University. In 1964, Dr. Oppenheim joined the faculty at MIT, where he is currently Ford Professor of Engineering and a MacVicar Faculty Fellow. Since 1967 he has been affiliated with MIT Lincoln Laboratory and since 1977 with the Woods Hole Oceanographic Institution. His research interests are in the general area of signal processing and its applications. He is coauthor of the widely used textbooks Discrete-Time Signal Processing and Signals and Systems. He is also editor of several advanced books on signal processing.

Dr. Oppenheim is a member of the National Academy of Engineering, a fellow of the IEEE, a member of Sigma Xi and Eta Kappa Nu. He has been a Guggenheim Fellow and a Sackler Fellow. He has also received a number of awards for outstanding research and teaching, including the IEEE Education Medal, the IEEE Centennial Award, the Society Award, the Technical Achievement Award and the Senior Award of the IEEE Society on Acoustics, Speech and Signal Processing. He has also received a number of awards at MIT for excellence in teaching, including the Bose Award and the Everett Moore Baker Award.